Accepted Manuscript

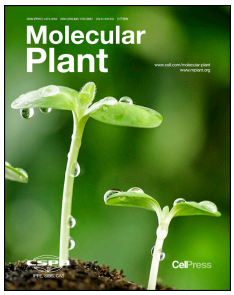

Arabidopsis Synaptotagmin 2 Participates in Pollen Germination and Tube Growth and is Delivered to Plasma Membrane via Conventional Secretion

Hui Wang, Shengcheng Han, Wei Siao, Chunqing Song, Yun Xiang, Xiaorong Wu, Pengyu Cheng, Hongjuan Li, Ján Jásik, Karol Mičieta, Ján Turňa, Boris Voigt, František Baluška, Jin Liu, Yingdian Wang, Heping Zhao

PII: S1674-2052(15)00364-0
DOI: 10.1016/j.molp.2015.09.003
Reference: MOLP 183

To appear in: *MOLECULAR PLANT*
Accepted Date: 5 September 2015

Please cite this article as: **Wang H., Han S., Siao W., Song C., Xiang Y., Wu X., Cheng P., Li H., Jásik J., Mi#ieta K., Tur#a J., Voigt B., Baluška F., Liu J., Wang Y., and Zhao H.** (2015). *Arabidopsis* Synaptotagmin 2 Participates in Pollen Germination and Tube Growth and is Delivered to Plasma Membrane via Conventional Secretion. Mol. Plant. doi: 10.1016/j.molp.2015.09.003.

Running title: SYT2 in Pollen Tube Growth

Arabidopsis Synaptotagmin 2 Participates in Pollen Germination and Tube Growth and is Delivered to Plasma Membrane via Conventional Secretion

Hui Wang[1⊙□], Shengcheng Han[1⊙], Wei Siao [2⊙], Chunqing Song[1⊙], Yun Xiang[3], Xiaorong Wu[3], Pengyu Cheng[1], Hongjuan Li[1], Ján Jásik[4], Karol Mičieta[5], Ján Turňa[6], Boris Voigt[2], František Baluška[2,7*], Jin Liu[1], Yingdian Wang[1] and Heping Zhao[1*]

1 Beijing Key Laboratory of Gene Resource and Molecular Development, College of Life Science, Beijing Normal University, 100875, Beijing, China

2 Department of Plant Cell Biology, IZMB, University of Bonn, Kirschallee 1, D-53115 Bonn, Germany

3 School of Life Science, Lanzhou University, 730000, Lanzhou, China

4 Comenius University Science Park, Comenius University, Bratislava, Mlynská dolina, 842 15 Bratislava 4, Slovakia

5 Department of Botany, Faculty of Natural Sciences, Comenius University, Révová 39, 811 02 Bratislava 1, Slovakia

6 Department of Molecular Biology, Comenius University, Faculty of Natural Sciences, Mlynská dolina, pavilion B-2, 842 15 Bratislava 4, Slovakia

7 Institute of Botany, Slovak Academy of Sciences, Dubravska cesta 9, SK-84523 Bratislava, Slovak Republic

⊙ These authors contributed equally to this work

□ Present address: Office of Teaching Affairs, Handan College, 056005, Handan, China

* Corresponding author: Heping Zhao (e-mail: hpzhao@bnu.edu.cn). Frantisek Baluska (e-mail: baluska@uni-bonn.de) contributed equally to this work.

The author responsible for distribution of materials integral to the findings presented in this article is: Heping Zhao (hpzhao@bnu.edu.cn).

Short Summary

Arabidopsis synaptotagmin 2 (*SYT2*), expressed mainly in *Arabidopsis thaliana* L. pollen, participates in pollen germination and tube growth. SYT2 was delivered to the plasma membrane from Golgi apparatus via conventional secretion. SYT2 binds to the membrane by means of C2 domains in a calcium-dependent manner.

ABSTRACT

Arabidopsis synaptotagmin 2 (SYT2) has been reported to participate in an unconventional secretory pathway in somatic cells. Our results showed that *SYT2* was expressed mainly in *Arabidopsis thaliana* L. pollen. The pollen of *syt2* T-DNA and RNA interference mutant lines exhibited reduced total germination and impeded pollen tube growth. The expression of SYT2-GFP fusion protein in the pollen tubes indicated that SYT2 was localised to distinct, patchy compartments and co-localised with the Golgi markers, BODIPY TR C5 ceramide and GmMan1-mCherry. The expression of SYT2-DsRed-E5 in *Arabidopsis* suspension cells demonstrated that the protein was localised to the plasma membrane, in addition to the Golgi apparatus. The localisation of SYT2 on the plasma membrane was supported by immunofluorescence staining in pollen tubes. Moreover, brefeldin A (BFA) treatment inhibited the transport of SYT2 to the plasma membrane and caused SYT2 to aggregate and form enlarged compartments. Truncation of the SYT2-C2AB domains also resulted in retention of SYT2 in the Golgi apparatus. An *in vitro* phospholipid-binding assay showed that SYT2-C2AB domains bind to the phospholipid membrane in a calcium-dependent manner. Given the aforementioned evidence, our results indicated that SYT2 was required for pollen germination and pollen tube growth, and was involved in conventional exocytosis.

Key words

Synaptotagmins, Pollen Germination, Pollen Tube, Tip Growth, Calcium-Dependent Phospholipid Binding, C2 Domains, Exocytosis, Conventional Secretion, Plant Polarity.

INTRODUCTION

The pollen tubes exhibit very rapid polar tip growth in which cell expansion occurs only at the extreme apex of the cell. During the tip growth, the tips of the pollen tubes undergo very active exocytosis to deliver the new components to the plasma membrane and the cell walls, as well as to secrete proteins via the Golgi apparatus-derived secretory vesicles (Camacho and Malhó, 2003; Chae and Lord, 2011; Moscatelli and Alessandra, 2013; Szumlanski and Nielsen, 2009). It was found that the tip-focused Ca^{2+} gradient is essential for the pollen tube growth and promotes the transport, priming and fusion of the secretory vesicles to the plasma membrane (Chen et al., 2015; Coelho and Malhó, 2006; Ge et al., 2007).

Synaptotagmins (Syt) constitute a family of membrane-trafficking proteins that regulate exo/endocytosis via membrane fusion in animal cells (Craxton, 2004; Jahn et al., 2003) and act as calcium sensors (Chapman, 2002; Tucker and Chapman, 2002). Syt1 is a synaptic-vesicle-localised protein that facilitates SNARE-catalysed membrane fusion in exocytosis after sensing Ca^{2+} influx (Apodaca, 2006; Martens et al., 2007; Tucker et al., 2004)). Syt2 plays an additional and non-redundant role in controlling synaptic transmission in Ca^{2+}-triggered neurotransmitter release, which is similar to the role of Syt1 (Leitzell, 2007; Pang et al., 2006). Syt7 has been proposed to regulate calcium-dependent membrane fusion of lysosomes in wound repair (Caler et al., 2001; Jaiswal et al., 2004; Martinez et al., 2000; Reddy et al., 2001). In addition, Syt7 has been reported to function as a Ca^{2+} sensor in calcium-induced glucagon exocytosis (Gustavsson et al., 2009). Syt1, Syt2 and Syt9 are known as Ca^{2+} sensors and modulate the fast synchronous neurotransmitter release (Xu et al., 2007). Syt9 regulates Ca^{2+}-dependent exocytosis in pancreatic islets and PC12 cells (Fukuda et al., 2002; Iezzi et al., 2005; Iezzi et al., 2004).

Seventeen isoforms of synaptotagmins have been reported in vertebrate animals (Bhalla et al., 2008). All synaptotagmins have a similar structure; an N-terminal transmembrane (TM) region, a linker of variable length, and two

tandem C2 domains, C2A and C2B (Craxton, 2007). The C2 domains, first identified in the second conserved regulatory domain of the classical protein kinase C (Cho and Stahelin, 2006; Coussens et al., 1986), are independently folded protein modules that bind to Ca^{2+} and phospholipids (Fernandez et al., 2001; Sutton et al., 1995). C2A and C2B domains of Syt1 are similar structures, consisting of compact β-sandwiches with eight β-strands connected by three flexible loops (Chapman, 2002; Fernandez et al., 2001). Five aspartic acid residues coordinating Ca^{2+} in loop1 and loop3 of each C2 domain of Syt1 are conserved only in a subset of synaptotagmins (Chapman, 2002; Koh and Bellen, 2003).

The *Arabidopsis* genome includes five genes that encode synaptotagmin-like proteins (Craxton, 2004). SYT1 (also called SytA) helps maintain the integrity of the plasma membrane when the membrane is disrupted by freezing (Yamazaki et al., 2008) and osmotic stress (Schapire et al., 2008). Another study illustrated SYT1 regulation of endocytosis and mediation of the transport of virus movement proteins between cells (Lewis and Lazarowitz, 2010; Uchiyama et al., 2014). SYT1 accumulates at the haustorial membrane around the invading oomycete *Phytophthora infestans* in *Nicotiana benthamiana* host leaf cells (Bozkurt et al., 2014; Lu et al., 2012). Moreover, SYT1 also accumulated in a fraction of detergent-resistant plasma membrane microdomains after cold acclimation (Minami et al., 2009; Takahashi et al., 2013) and was detected as an interacting partner of the brassinosteroid receptor kinase BRI1 (Wang et al., 2013). A recent study also demonstrated that *Arabidopsis* SYT1 is an ER-PM contact sites component which maintains the mechanical stability of the cells (Perez Sancho et al., 2015). Surprisingly, synaptotagmin and the eyespot assembly proteins EYE3 and SOUL3 have recently been reported in the plastoglubuli proteome of halotolerant green algae *Dunaliella* (Davidi et al., 2014). Finally, synaptotagmin was involved in rhizobia-legume symbiosis in *Medicago* spp. (Rose et al., 2012), and in roots of *Robinia pseudoacacia* entering symbiosis with *Mesorhizobium amorphae* (Chen et al., 2013).

The 35S promoter-driven overexpression of SYT2 in *Arabidopsis* leaf and root cells showed SYT2 localisation to the Golgi apparatus and involvement in regulation of unconventional secretion of hygromycin B phosphotransferase (Zhang et al., 2011). However, the intrinsic physiological role of SYT2 in *Arabidopsis* has not been determined.

In this study, we have demonstrated that SYT2 is expressed mainly in pollen and localise to the Golgi apparatus. SYT2 is delivered to the plasma membrane via brefeldin A (BFA)-sensitive secretory vesicles. The C2 domains of SYT2 play a crucial role in directing SYT2 to the plasma membrane. To our knowledge, SYT2 is the first *Arabidopsis* synaptotagmin demonstrated to participate in conventional secretion and play a role in pollen germination and pollen tube tip growth.

RESULTS

Arabidopsis SYT2 is Expressed Mainly in Pollen Grains

To understand the physiological role of *Arabidopsis SYT2*, we analysed *SYT2* gene expression in various organs using a gene-specific RT-PCR and a promoter: GUS reporter system. The result of real-time PCR showed that *SYT2* was expressed mainly in freshly harvested and non-hydrated pollen grains, whereas its expression was relatively very low in roots, stems, leaves and siliques (Fig. 1A). The results of semi-quantitative RT-PCR also indicated a high level of *SYT2* transcript in the inflorescence and stamens (Supplemental Fig. 1).

In a tissue-specific expression study of *SYT2*, a native *SYT2* promoter was fused to a GUS reporter gene and introduced into wild-type *Arabidopsis*. Two independent lines of *pSYT2:GUS* transgenic *Arabidopsis* (made by two different laboratories) were selected for an intermediate level of gene expression from a transgenic population according to quantitative fluorometric and qualitative histochemical GUS analyses. The histochemical and fluorometric GUS assay showed that the highest GUS activity was in the inflorescence (Fig. 1B; Supplemental Fig. 2A). Quantitative analysis of *SYT2* promoter activity was conducted using one of the transgenic lines and showed that maximum activity was in flower buds, shortly before anthesis (Fig. 1C), and the strongest signal was in stamens and, to a lesser extent, pistils (Fig. 1D).

Detailed histochemical examination suggested that the GUS staining was limited to developing female gametophytes (unfertilised embryo sacs, Fig.1E) and developing male gametophytes (pollen grains, Fig. 1F; Supplemental Fig. 2B). The growing pollen tubes showed strong GUS staining under *in vitro* conditions (Fig. 1G). Since GUS staining was present both in ovules and pollen tubes, we performed reciprocal crossing of the *pSYT2*:*GUS* transgenic line with wild type *Arabidopsis* to discriminate these two signals after pollination. No GUS staining was observed in the wild type ovules after pollination with transgenic pollen grains; nevertheless, the staining of transgenic pollen tubes was evident in the pistils (Fig. 1H). These data suggested that *SYT2* was also expressed in pollen tubes grown

in vivo in pistils. On the other hand, after the pistils of transgenic plants were pollinated by pollen from wild-type plants, GUS staining of the fertilised and enlarged ovules became weaker and disappeared (Fig. 1I), while the unpollinated ovules remained small and strongly stained (Fig. 1J). These results suggested that *SYT2* could play a role in the development of embryo sacs and pollen grains, as well as in the pollen germination and tip growth of pollen tubes.

SYT2 Mutants Show Decreased Total Pollen Germination Percentages and Pollen Tube Lengths Compared with WT Pollen Tubes

We have obtained three *Arabidopsis* mutants, named *syt2-1*, *syt2-2*, and *syt2-3*, from the SALK collection (i.e., SALK_133731, SALK_016690, and SALK_072947) with T-DNA located in the second intron, the ninth exon, and another position of the ninth exon of At1G20800, respectively (Fig. 2A). Mutant lines with different T-DNA insertion sites on the *SYT2* locus were screened by genomic PCR with *SYT2* and T-DNA border-specific primers (Supplemental Table 1).

The genotyping results are shown in Fig. 2B. The level of the *SYT2* transcript in *syt2-2* was very low and could not be detected by RT-PCR. *Syt2-1* and *syt2-3* only showed a trace amount of SYT2 transcripts (Fig. 2C).

Arabidopsis RNAi lines were also generated to investigate the function of *SYT2* (Supplemental Fig. 3). One SYT2-RNAi line with reduced *SYT2* (*RNAi-#5*) expression was identified by RT-PCR (Fig. 2C) and used for further investigation of phenotype.

Pollen germination percentages of the homozygous T-DNA insertion mutants (*syt2-1*, *syt2-2* and *syt2-3*) and an RNAi line (*RNAi-#5*) were calculated and compared with the wild type by *in vitro* means of germination assays. Results showed that the relative germination efficiency of pollen from T-DNA mutants ranged from 54.6 to 78.2% at 5 hours after imbibition, and the relative germination efficiency of pollen from the *RNAi-#5* line was 52.0% (Fig. 2D). We also calculated the germination percentages at 6.5 h after imbibition, and the data showed that both the *SYT2* mutants and wild type pollen grains already

reached their maximal germination percentages after 5 h of imbibition (Supplemental Table 2). The final pollen germination percentages of *SYT2* mutants were lower than that of wild type. These results indicated that *SYT2* contributed to pollen viability.

To determine whether the mutation of *SYT2* gene affected pollen tube elongation, we measured the lengths of pollen tubes of wild-type and mutant lines germinated for 5 h on *in vitro* medium. Average lengths of the pollen tubes were 115 μm in the wild type and from 77 to 100 μm in the mutants (Fig. 2E). The homozygous *syt2-1*, *syt2-2*, *syt2-3* and *RNAi-#5* lines represented a 13.1%, 18.3%, 25.2% and 32.2%, respectively, reduction in the average length of pollen tubes. More than 66% of wild-type pollen tubes were longer than 95 μm and only 0.3% were shorter than 55 μm. The mutants had a markedly lower percentage of pollen tubes longer than 95 μm, compared with the wild type. The proportions of pollen tubes <55 μm were considerably higher in the mutant lines, especially the RNAi mutant. We found 30.9% of *RNAi-#5* pollen tubes to be <55 μm (Fig. 2E). We also measured the lengths of pollen tubes from 1 h to 3 h, and the results showed that the pollen of *SYT2* mutants had already germinated and grown much the same lengths as that of wild type at 1 h (Supplemental Fig. 4). However, the growth rates of pollen tubes of *SYT2* mutants were slower than that of wild type after 1h. In addition, the growth rates of pollen tubes of both wild type and the mutant lines were very slow after 5 h of imbibition, but the growth rate of *SYT2* mutant was still lower than that of wild type (Supplemental Table 2). Taken together, we showed that the shorter pollen tubes of *SYT2* mutants were not due to the delayed germination but the retarded elongation.

These data demonstrated that the *SYT2* gene also played a role in elongation of pollen tubes. Although the pollen tubes of *SYT2* mutants were shorter than wild-type pollen tubes, the mutants exhibited sufficient pollen tubes long enough to accomplish fertilization, which may explain the lack of a marked difference in seed setting percentage between the mutants and

wild-type plants.

SYT2-GFP is Localised Mainly to the Golgi Apparatus

To evaluate the subcellular localisation of SYT2, two plant expression systems were used, including stable expression of SYT2-GFP driven by a *pLAT52* promoter in transgenic *Arabidopsis* and transient expression of SYT2-GFP in tobacco (*Nicotiana tabacum* L.) pollen grains by microparticle bombardment with a *pLAT52:SYT2-GFP* construct. Both the results showed that the SYT2-GFP fusion protein was localised to distinct patches in the growing pollen tubes, but rarely to the plasma membrane (Fig. 3; Supplemental Fig. 5Aa and 5Ac). In stable transgenic *pLAT52:SYT2-GFP Arabidopsis*, the SYT2-GFP-containing compartments were co-localised with the Golgi dye BODIPY TR C5 ceramide (B-34400, Invitrogen) and the Golgi marker GmMan1-mCh, the cytoplasmic tail and transmembrane domain of GmMan1 fused with mCherry (Nelson et al., 2007), which was transiently expressed by particale bombardment but not the endocytic vesicle marker FM4-64 and the ER-Tracker Blue-White DPX (Fig. 3A). To further examine the subcellular localisation of SYT2-GFP, we treated the pollen tubes with the secretion inhibitor BFA (35.6 μM) and the late endosomes/autophagy inhibitor wortmannin (10 μM) for 30 min after 3 h of germination. The results showed that SYT2-GFP formed enlarged aggregates after BFA treatment and decorated around the FM4-64-stained BFA compartments featuring the Golgi localisation of SYT2-GFP (Fig. 3B). Wortmannin slightly changed the morphology of SYT2-GFP vesicles in the pollen tubes, but SYT2-GFP was not accumulated into the wortmannin-induced multivesicular compartments indicating that SYT2-GFP was not localised to the trans-Golgi network and the prevacuoles (Fig. 3B).

As a control, the cytosolic GFP protein alone showed diffuse distribution in the cytoplasm and nucleus in tobacco pollen tubes (Supplemental Fig. 5Ab). The results of transiently transforming *pLAT52:SYT2-GFP* and *pLAT52:GFP* into tobacco pollen showed similar results to those in *Arabidopsis* (Fig. 3C).

To confirm the subcellular localisation of SYT2 in pollen tubes, we performed

immunofluorescence labelling of SYT2 using a SYT2-specific antibody. The results indicated that SYT2 was localised not only to the Golgi apparatus but also to the plasma membrane in pollen tubes (Supplemental Fig. 6). However, since the SYT2-GFP fluorescence signal was very weak on the margin of transgenic pollen tubes, it was difficult to determine if SYT2 was located on the plasma membrane or the endocytosis-derived vesicles in pollen tubes.

SYT2 is Transported from the Golgi Apparatus to the Plasma Membrane

To confirm that SYT2 was localised to the plasma membrane, we first examined the subcellular localisation of SYT2 by expressing SYT2-GFP in *Arabidopsis* suspension cells, and found that the SYT2-GFP signal had a patchy distribution around the nucleus in suspension cells, whereas GFP alone showed diffuse localisation in the cytosol and inside the nucleus (Supplemental Fig. 5B). However, the SYT2-GFP signal near the plasma membrane in suspension cells was too weak to be imaged clearly.

Previous studies showed that DsRed-E5 changes its fluorescence colour over time, shifting from green to red fluorescence after maturation. The ratio of green to red fluorescence can be used to estimate the age of the fusion protein (Mirabella et al., 2004; Terskikh et al., 2000). Therefore, we employed DsRed-E5 to label SYT2 and established the stably transformed *Arabidopsis* suspension cell line expressing *SYT2-DsRed-E5* driven by a *35S* promoter. The SYT2-DsRed-E5 fusion protein in suspension cells displayed a patchy distribution similar to that of SYT2-GFP in tobacco and Arabidopsis pollen tubes. Moreover, SYT2-DsRed-E5 fluorescence signal was also clearly detected on the plasma membrane in the red fluorescence channel (Fig. 4A), while DsRed-E5 alone was diffusely distributed in the cytoplasm and inside the nuclei (Supplemental Fig. 5C). A z-stack projection of the images in Fig. 4A is shown in Fig. 4B. By comparing the fluorescent lines on the cell periphery (indicated by arrows in Fig. 4A and 4B) with the non-fluorescent trans-vacuolar cytoplasmic strands (indicated by arrows in Fig. 4C), we inferred that the fine fluorescent lines were not on the tonoplast, but on the plasma membrane. In addition, the plasmolysis

assay indicated that SYT2 was not localised to the cell wall (Fig. 4D).

Detailed analysis of the punctate structures around the nucleus revealed that these spots emitted both green and red fluorescence. Moreover, green fluorescence on the punctate structures around the nucleus was considerably stronger than that on the plasma membrane, while the red fluorescence showed a less marked difference (Fig. 4A, 4C). This result indicated that the SYT2-DsRed-E5 proteins localised to the Golgi apparatus around the nucleus were newly synthesised and those localised to the plasma membrane represented the older SYT2-DsRed-E5 population.

To further characterise the spatiotemporal dynamics of SYT2-DsRed-E5, we performed quantitative analysis and calculated the ratio of green to red fluorescence intensity on vesicles around the nuclei (V_1), vesicles near the plasma membrane (V_2), and the plasma membrane (M) from the original grayscale images (Fig. 5A). As shown in Fig. 5B, the green fluorescence on both V_1 and V_2 vesicles was stronger than the red fluorescence, as the green/red signal ratio of V_1 was 7.6/1 and that of V_2 was 6.8/1 (Fig. 5B). Red fluorescence on the plasma membrane was stronger than the green fluorescence, as the green/red signal ratio of the plasma membrane was 1/5.2 (Fig. 5B). The intensities of green and red fluorescence signals of DsRed-E5 alone in the cells were similar, with a green/red signal ratio of 1.7 (Fig. 5B). A previous study reported that a red/green ratio ≥ 1 indicated that the DsRed-E5 protein was produced more than 10 h ago *in vitro* and in *Caenorhabditis elegans* cells (Terskikh et al., 2000), and approximately more than 30 h in cowpea mesophyll protoplasts (Mirabella et al., 2004). This indicated that the majority of SYT2-DsRed-E5 proteins on the plasma membrane had been synthesised at least 10 h previously, which demonstrated that the SYT2 protein was transported from the Golgi apparatus to the plasma membrane over time.

SYT2 is Transported to the Plasma Membrane via Conventional Secretion

We further examined the localisation of SYT2-DsRed-E5 in the suspension

cells after treatment with the secretion inhibitor BFA. Compared with untreated cells, cells treated with BFA for 20 and 40 min displayed enlarged SYT2 vesicle aggregates, and the fluorescence signal of SYT2-DsRed-E5 on the plasma membrane was reduced (Fig. 6; Supplemental Fig. 7). Quantitative analyses of the green/red fluorescence signal ratio of the vesicles and plasma membrane at different time points with BFA treatment are shown in Fig. 6D. The results showed that the green/red fluorescence ratio of vesicles decreased over time following treatment with BFA. For the plasma membrane, the green/red fluorescence ratio was increased after BFA treatment (Fig. 6D). The intensities of DsRed-E5 green and red fluorescence signals in the suspension cells were approximately the same (Fig. 6D).

These results suggested that the newly synthesised SYT2-DsRed-E5 protein was mainly incorporated into the BFA compartments and was not transported to the plasma membrane, whereas old SYT2-DsRed-E5 protein seemed to be retained on the plasma membrane. The results showed clearly that SYT2 was transferred to the plasma membrane via the conventional secretory pathway in *Arabidopsis* suspension cells.

C2 Domains are Crucial for Localisation of SYT2 to the Plasma Membrane

Arabidopsis SYT2 contains two C2 domains, C2A and C2B. C2A was 62.4% similar to SYT1 and C2B was 73.5% similar to SYT1 (Supplemental Table 3). To characterise the role of C2 domains in the localisation of SYT2, we created a potential dominant-negative *SYT2* mutant lacking the C2A and C2B domains (*SYT2*$^{\Delta C2AB}$). Similar to SYT2-GFP, SYT2$^{\Delta C2AB}$-GFP accumulated in distinct patches in the cytoplasm (Fig. 7A) and was highly co-localised with the C5-ceramide-stained Golgi apparatus (Fig. 7B). SYT2$^{\Delta C2AB}$-DsRed-E5 also showed distinct patchy distribution in the cytoplasm (Fig. 7C), and there was no obvious difference between the distributions of SYT2$^{\Delta C2AB}$-GFP and SYT2$^{\Delta C2AB}$-DsRed-E5. However, unlike the full length of SYT2-DsRed-E5 (Fig. 4), only a trace amount of SYT2$^{\Delta C2AB}$-DsRed-E5 red fluorescence was

detected on the plasma membrane (Fig. 7C). These results suggested that the C2 domains of SYT2 played a role in directing SYT2 to the plasma membrane.

The C2 Domains of SYT2 Show Calcium-dependent Phospholipid Binding

We further investigated whether the C2 domains of SYT2 could bind to the negatively charged liposomes (25% PS/75% PC), and found that the SYT2-C2A peptide was able to bind a phospholipid in a calcium-dependent manner (Fig. 8A). The maximum concentration of free Ca^{2+} binding to SYT2-C2A was 7 μM, and a higher calcium ion concentration did not increase binding of SYT2-C2A to the liposomes. Moreover, binding of SYT2-C2B to the liposomes was calcium-independent (Fig. 8B). SYT2-C2B was associated with liposomes in the absence of free Ca^{2+}, and this binding was not enhanced by increased calcium concentration. The binding property of SYT2-C2AB differed from those of the two individual domains; indeed, SYT2-C2AB behaved as an approximate mixture of C2A and C2B. Half-maximal binding of C2AB to phospholipids was approximately 2 to 3 μM of free Ca^{2+} (Fig. 8C), while that of C2A was about 4 to 5 μM (Fig. 8A). As controls, all the C2 domains of SYT2 were subjected to different concentrations of Na^{+} and Mg^{2+}. The effects of Na^{+} (Supplemental Fig 8) and Mg^{2+} (Supplemental Fig 9) on the binding of SYT2 C2 domains with liposomes were found to be insignificant. These data indicated that the C2 domains of SYT2 were bound to phospholipids in membranes and that this binding was regulated by calcium ions.

DISCUSSION

SYT2 belongs to a small gene family. In the *Arabidopsis* database (i.e. TAIR), there are five *SYT* genes containing one transmembrane domain and two C2 domains (Craxton, 2004). These genes may share a common ancestral gene, as the exon-intron structures among the *SYT* genes are highly conserved (Yamazaki et al., 2010). Unlike the ubiquitous expression of *SYT1* in *Arabidopsis*, we clearly demonstrated by promoter analysis that *SYT2* was expressed mainly in the female and male gametophytes of *Arabidopsis,* especially in the developing embryo sacs, pollen grains and the growing pollen tubes (Fig. 1A, 1F, 1G). Semi-quantitative RT-PCR analysis also showed that *SYT2* was highly expressed in stamens, particularly in pollen grains. Both the results from promoter and RT-PCR analyses are in agreement with the microarray data for At1G20080 gene available from the Genevestigator database (https://www.genevestigator.ethz.ch) (Zimmermann et al., 2004). All these data suggest that *SYT2* plays a specific role in the development and growth of female and male gametophytes.

Subcellular localisation of synaptotagmins is essential to determine protein functions (Schapire et al., 2008). Previous reports showed that mammalian Syt1 and Syt7 are localised to synaptic vesicles and lysosomes, respectively, and are proposed to be Ca^{2+} sensors regulating the neurotransmitter release and/or resealing of the plasma membrane (Brose et al., 1992; Reddy et al., 2001).

In this study we found that SYT2-GFP was localised to the Golgi apparatus with a patchy distribution in *Arabidopsis* suspension cells, as well as in pollen tubes, which was in accordance with (Zhang et al., 2011)). More information on the localisation of SYT2 was obtained when SYT2 was fused with the fluorescent protein timer DsRed-E5 and expressed in suspension cells. SYT2-DsRed-E5 was localised to the plasma membrane as well as in distinct patches around the nuclei. This fluorescent timer showed that the newly synthesised SYT2 was first localised on the Golgi apparatus, and then

transferred to the plasma membrane. Furthermore, the C2 domains were necessary to transport SYT2 from the Golgi apparatus to the plasma membrane. The secretion inhibitor BFA also prevented the transport of SYT2 to the plasma membrane. These results are similar to the description of the molecular function of animal synaptotagmins, which act as Ca^{2+} sensors and trigger fusion of secretory vesicles with the plasma membrane.

Previous studies showed that *Arabidopsis* SYT1-GFP was localised mainly on the plasma membrane (Lewis and Lazarowitz, 2010; Schapire et al., 2008; Yamazaki et al., 2008), while *Arabidopsis* SYT2-GFP was rarely observed on the plasma membrane both in our study and in a previous report (Zhang et al., 2011). A recent paper also indicated that *Arabidopsis* SYT1-GFP is anchored at the ER, but not the plasma membrane, and was localised on the stationary ER-PM contact sites (Perez Sancho et al., 2015), while in our results SYT2-GFP and SYT2-DsRed-E5 were localised on the motile Golgi apparatus. These results provide evidence for the two SYTs playing different roles in *Arabidopsis*. SYT1 is required to maintain the integrity of plasma membranes during freezing conditions (Yamazaki et al., 2008), osmotic stress (Schapire et al., 2008) and mechanical stress (Perez Sancho et al., 2015). On the other hand, SYT2 is required for pollen tube tip growth and for the pollen viability. This implies that SYT2 may facilitate the constitutive secretion of substances to the plasma membrane and/or to the extracellular space that is important for pollen development and for pollen tube elongation.

It is interesting that SYT2-GFP signals were not detected on the plasma membrane in pollen tubes (Fig. 3), suspension cells (Supplemental Fig. 5) and root cells (Zhang et al., 2011), but SYT2-DsRed-E5 and anti-SYT2 antibody labelled both the Golgi apparatus and the plasma membrane (Fig. 4 to 7 and Supplemental Fig. 6). GFP (27 kDa) from the jellyfish *Aequorea victoria* has the similar molecular weight and topology with DsRed monomer (28 kDa) from a coral of the *Discosoma* genus (Chudakov et al., 2010; Terskikh et al., 2002). However, DsRed shows a slow rate of fluorescence development and forms

an obligate tetramer *in vitro* and in living cells (Baird et al., 2000; Yarbrough et al., 2001). We are proposing two possible scenarios explaining why SYT2-GFP cannot be transferred to the plasma membrane. Firstly the chemical property of GFP interrupts the interactions between the C2 domains of SYT2 and the plasma membrane or other protein components that are essential for the membrane fusion process. On the other hand, the effect of DsRed-E5 is less noticeable. Secondly, the clustering or oligomerisation of SYT2 proteins are necessary for the attachment or fusion of the SYT2-localised vesicles to the plasma membrane. Fusion of GFP to the C terminus of SYT2 prevents this oligomerisation while DsRed-E5 compensates this disruption by forming a tetramer and brings SYT2 close enough to function properly in exocytosis. Since exocytosis can be divided into three steps: docking, priming and release, further studies on how SYT2 interact with other components may provide better understanding of the roles of SYT2 in exocytosis. Furthermore, we cannot exclude the possibility that DsRed-E5 also affects the endocytosis for recycling the SYT2 back from the plasma membrane. More protein interactome analysis would be helpful to reveal the function of SYT2 in exocytosis/endocytosis.

The functions of *Arabidopsis* synaptotagmins are often inferred from animal synaptotagmins, based on the similarity of the sequences and domain architectures. However, there is no direct evidence that plant synaptotagmins mediate membrane fusion in cells. This may be due to the difficulty in establishing a plant membrane fusion test system *in vivo* (Zarsky et al., 2009). Therefore, alternative methods must be used to obtain circumstantial evidence. The *in vitro* phospholipid-binding assay is a well-established system of determining whether a protein binds to phospholipid bilayers in a calcium-dependent or -independent manner. The Ca^{2+}-binding affinity of animal Syt1, determined *in vitro*, is similar to the physiologically relevant concentrations in cells (Geppert et al., 1994).

In plant pollen tubes, intracellular Ca^{2+} shows a tip-focused distribution (Gu et

457 al., 2003). For example, cytosolic Ca^{2+} concentrations in lily pollen tubes
458 decline drastically from 3–5 μM at the extreme apex to basal levels (100–200
459 nM) within 20 μm (Hepler et al., 2001; Pierson et al., 1994). This tip-focused Ca^{2+}
460 gradient is required for pollen tube elongation, as it may facilitate fusion of
461 secretory vesicles with the plasma membrane (Helling et al., 2006; Hepler et al.,
462 2001)).

463 In this report, the C2A domain of SYT2 acted as a Ca^{2+}-dependent
464 phospholipid-binding domain, while the C2B domain had Ca^{2+}-independent
465 phospholipid binding activity. The phospholipid binding property of the C2AB
466 domain was also calcium-dependent, with half-maximal binding occurring at
467 2–3 μM free Ca^{2+} (Fig. 8). This calcium-dependent binding property of SYT2 is
468 correlated with the maximal calcium concentration at the pollen tube tips and
469 supports the physiological function of SYT2 on transporting the secretory
470 vesicles to the plasma membrane in the rapid growing pollen tubes.

471 The N-terminal transmembrane domain of synaptotagmin is inserted into the
472 membrane of secretory vesicles, and the C2 domains can bind to the target
473 membrane under regulation of Ca^{2+} (Jefferson et al., 1987). Our results showed
474 that the C2 domains of SYT2 were important for the localisation of SYT2 to the
475 plasma membrane (Fig. 7C). However, the N-terminal transmembrane domain
476 (amino acids 2 to 26) of SYT2 alone was sufficient for proper localisation of SYT2
477 on the Golgi apparatus. This indicated that the transmembrane domains
478 determined the localisation of SYT2 on the Golgi apparatus, while the C2
479 domains facilitated its transfer to the plasma membrane.

480 The vitality of pollen grains has a marked effect on germination and growth of
481 pollen tubes (Fan et al., 2001). The vigour of plants and flowers affects the
482 vitality of their pollen grains. To minimise the differences in pollen vitality due to
483 the differences in vigour of wild-type and mutant plants, flowers were selected
484 according to strict criteria. In this study, we identified three T-DNA insertion
485 mutants (*syt2-1*, *syt2-2*, and *syt2-3*) and obtained an RNAi mutant of *SYT2*.
486 *SYT2* mutations resulted in the reduction of pollen germination and shorter

pollen tubes compared to the wild type (Fig. 2D, 2E). The loss-of-function mutants of *SYT2* had a slower rate of pollen tube growth (Supplemental Fig. 4 and Table 2). This phenotype was not obvious, and this experiment could be repeated only with very strict selection of flowers and plants.

This result implied that *SYT2* mutations had a slight effect on the growth of pollen tubes, while other factors, such as health of the plants, may have influenced pollen viability. The weak phenotype of *SYT2* mutants may have been due to gene redundancy, since four other synaptotagmin genes (e.g., *SYT1*) could also be expressed in *Arabidopsis* pollen; these may compensate for the functional deficiencies of *SYT2*.

Arabidopsis SYT2 has been reported to play a role in unconventional secretion (Zhang et al., 2011). The proteins involved in unconventional secretion lack the typical N-terminal signal peptides and the export processes are not inhibited by BFA (Duran et al., 2010). For pollen tubes, our data showed that BFA inhibited transport of SYT2 to the plasma membrane and disrupted the normal localisation of SYT2 on the Golgi apparatus in suspension cells (Fig. 6). In the tip-growing pollen tubes, SYT2 was involved in conventional secretion. This may be due to differences in the cell culture systems. We used pollen tubes and suspension cell cultures for subcellular localisation, while a previous report used root cells and protoplasts (Zhang et al., 2011). Our study provides a new perspective for research on the role of SYT2 in *Arabidopsis* pollen tube growth and the function of the conventional secretory pathway.

MATERIALS AND METHODS

Plant Growth Conditions

Arabidopsis (Col-0) seeds were planted in pots, at a 3:1 nutritional soil vermiculite mix. After 2 d at 4℃, the seeds were g rown with supplemental lighting (16-h photoperiod at 120–150 μmol/m^2/s at 22℃; (Fan et al., 2001). Seeds of T-DNA insertion lines and RNAi transgenic lines were disinfected with 1% sodium hypochlorite and washed with sterile water, and then sown in Murashige and Skoog medium with 0.8% agar (Lalanne et al., 2004). The 2-week-old seedlings were then transferred to pots and grown for 4 weeks under the light conditions described above.

T-DNA Insertion Line

The *Arabidopsis* T-DNA insertion lines (SALK_133731, SALK_016690, and SALK_072947, identified as *syt2-1*, *syt2-2*, and *syt2-3*, respectively) were obtained from the SALK T-DNA collection. Homozygosity of mutant lines was confirmed by PCR analysis of genomic DNA, using the specific primers listed in Supplemental Table 1. The expression of the *SYT2* gene in the homozygous mutant lines was determined by RT-PCR. PCR products were verified by sequencing.

RNAi Transgenic Lines

The sense and antisense DNA fragments of the *SYT2* exon, amplified using specific primers (Supplemental Table 1), were subcloned into pFGC1008. The construct was transformed into the *Arabidopsis* genome using the *Agrobacterium tumefaciens*-mediated method. Hygromycin-resistant transgenic *Arabidopsis* plants were screened and confirmed by genomic PCR analysis by amplifying the GUS segment of pFGC1008. The expression of *SYT2* in transgenic plants was confirmed by RT-PCR using the primer sets for real-time PCR (Supplemental Table 1).

RNA Isolation and RT-PCR

Total RNA was isolated from various plant tissues using the TRIzol® reagent (Invitrogen), according to the manufacturer’s instructions. A quantity of 5-μg

539 total RNA was used for reverse transcription with the RevertAid First Strand
540 cDNA Synthesis Kit (Fermentas), according to the manufacturer's instructions.
541 Real-time PCR analysis was conducted using the SYBR® Green PCR Master
542 Mix (ABI), referring to the manufacturer's instructions. The data were processed
543 using the 7000 SDS software. The *Actin2* gene was used as an internal control
544 (Nicot et al., 2005; Thorlby et al., 2004). The specific primers for each gene are
545 listed in Supplemental Table 1. This experiment was conducted three times
546 independently, and the means and standard deviations were calculated. For
547 semi-quantitative RT-PCR, PCR analysis was performed on 15 µL using the
548 GoTaq® Hot Start Polymerase (Promega, Mannheim, Germany) on an
549 Eppendorf Mastercycler Pro instrument (Eppendorf). The following
550 amplification program was used: one cycle at 95℃ for 3 min, 35 cycles for
551 SYT2 gene and 30 cycles for reference genes at 95℃ for 15 s, 56℃ for 30 s,
552 73℃ for 30 s, and then one cycle at 73℃ for 5 min . The primers are listed in
553 Supplemental Table 1. Band intensities were analysed using the Image J
554 software. This experiment was repeated twice independently.

555 ***SYT2* promoter activity analysis**

556 A fragment of 2014 bp, upstream from the start codon in the gene At1G20080,
557 was amplified using the primers listed in Supplemental Table 1 and cloned into
558 the expression vector pCAMBIA1305.1, and then transformed into *Arabidopsis*
559 by *Agrobacterium tumefaciens*. Homozygous lines were obtained and the
560 histochemical GUS assays were performed as described (Jefferson et al.,
561 1987). Protein was extracted with 50 mM phosphate buffer (pH 7.3)
562 supplemented with 10 mM EDTA, 0.1% (v/v) Triton X-100, 0.1% (w/v) SDS,
563 and 10 mM dithiothreitol. The fluorometric analysis reaction was performed in
564 black 96-well microtiter plates (NUNC, Germany) in darkness at 37℃. The
565 50-µL extraction buffer contained 1 mM MUG as a substrate and 1 µg of total
566 protein. After one hour, the reaction was stopped by addition of 150-µL
567 carbonate buffer (200 mM) and fluorescence intensity was measured using a
568 multidetection Tecan Infinite M20 microplate reader (Tecan Trading AG) with

362 (±9)-nm excitation and 450 (±20)-nm emission. Protein concentration was measured using the Lowry-based Bio-Rad DC protein assay (Bio-Rad, Germany).

In vitro Pollen Germination and Tube Length Measurements

Pollen grains from freshly anther-dehisced flowers of wild-type and mutant *Arabidopsis* plants were germinated in 35-mm petri dishes at room temperature for 5 h on basic medium (20% sucrose, 5 mM boric acid, 8 mM $MgSO_4$, 5 mM $CaCl_2$, 1 mM KCl, 10 mM inositol, and 5 mM MES-KOH, pH 7.0; (Fan et al., 2001), and observed using a Zeiss Observer Z1 microscope. At least 100 pollen tubes were chosen randomly for length measurements using Axio software (vision 4.0). Pollen germination in this study refers to the length of pollen tube exceeding half the pollen diameter. Average lengths and standard errors over several hundred pollen tubes were computed. All experiments were repeated at least three times. All the fluorescent dyes and inhibitors were diluted in the basic medium with the indicated final working concentrations in the figure legends.

Generation and Purification of GST Fusion Proteins

DNA sequences encoding the C2A domain of SYT2 located from amino acids 244 to 400, the C2B domain (401 to 537) and C2AB tandem (247 to 537), were ligated into a pGEX-2z vector. Purification of GST fusion protein was carried out as described previously (Guan and Dixon, 1991; Schapire et al., 2008).

Phospholipid Binding Assays

Binding of C2 domains (C2A, C2B and C2AB) of SYT2 to phospholipids was measured according to previous descriptions (Fernandez-Chacon et al., 2002; Fernandez et al., 2001; Schapire et al., 2008; Shin et al., 2003). Phospholipids (PS/PC = 25/75, w/w; Avanti polar Lipid) were used in this experiment. Calcium concentrations were calculated using the Winmaxc32 (version 2.51) software downloaded from http://www.stanford.edu/~cpatton/downloads.htm. The proteins were detected by SDS-PAGE. The Coomassie Brilliant Blue-stained gels were scanned using Bio-Rad ChemiDoc XRS and then analysed using the

Quantity One software.

Transformation of Tobacco and *Arabidopsis* Pollen Grains Using Particle Bombardment

Tobacco was planted in a controlled growth chamber at 25℃ with 16-h daylight. The pollen grains were collected from anthers that had not dehisced on SR1 flowers. All plasmid DNA was prepared using the UltraClean Endotoxin-Free Maxi Plasmid Prep Kit (Beijing ZEPING Bioscience). Golgi marker GmMan1-mCherry (G-rk, CD3-967) was purchased from the Arabidopsis stock centre (http://www.arabidopsis.org). A quantity of 10 mg of mature pollen grains was used in each bombardment. Pollen germination medium (0.01% H_3BO_3, 1 mM $MgSO_4$, 5 mM $CaCl_2$, 5 mM $Ca(NO_3)_2$, 18% sucrose, and 20 mM MES, pH 6.5-7.0) was prepared to incubate pollen grains (Fan et al., 2001). Pollen suspension was spotted and solidified on a nylon membrane in 90-mm petri dishes. Gene bombardment was performed using the helium-driven PDS-1000/He system (Bio-Rad). Plasmid DNA, 0.1 M spermidine, and 2.5 M $CaCl_2$ were attached to gold particles (1 μm), according to the Bio-Rad manual (Chen et al., 2002; Sanford et al., 1993). A total of 3 mg of DNA was used to coat 1 mg of gold particles. Each prepared simple was twice bombarded toward an individual pollen sample to improve the frequency of transformation. Bombardments were performed under the following conditions: 28-inch Hg chamber vacuum, 1100-psi rupture disc, 0.25-inch gap distance, and 1-inch particle travel distance. Boomed pollen grains were washed from the nylon membrane using germination medium and germinated in 35-mm petri dishes with shaking at 60 rpm in the dark. Pollen tubes were observed using an Olympus FV300-IX700 laser scanning confocal microscope. Images were analysed using an FV1000 viewer (version 1.6).

Transformation of *Arabidopsis* Callus Cells

Stable transformation of *Arabidopsis* callus (induced from seeds of Col-0 ecotype) was performed using *Agrobacterium tumefaciens* (strain GV3101) according to methods described previously (Dhonukshe and Gadella, 2003).

The plant expression vector pCAMBIA1300.1, containing *35S-SYT2-GFP-tNOS*, *35S-SYT2$^{\Delta C2AB}$-GFP-tNOS*, *35S-GFP-tNOS*, *35S-SYT2-DsRed-E5-tNOS,* *35S-SYT2$^{\Delta C2AB}$-DsRed-E5-tNOS*, and *35S-DsRed-E5-tNOS* constructs, was used for transformation.

Microscopy

Confocal microscopy was performed using an Olympus FV-300-IX70 confocal laser scanning microscope. ER-Tracker Blue-White DPX was excited with the diode laser (405 nm) and the emission was detected between 425 and 475 nm. GFP was excited with the blue argon ion laser (488 nm), and emitted light was collected through a 510-nm long-pass filter. The red fluorescent dyes FM4-64 and BODIPY TR C5 ceramide (B-34400, Invitrogen) were excited with a green HeNe laser (543 nm), and emitted light was collected through a 620-nm band-pass filter. The excitation/emission wavelengths of DsRed-E5 were 483/500 nm for green fluorescence and 558/583 nm for red fluorescence. Differential interference contrast microscopy images were collected synchronously. Images were analysed using an Olympus FV1000 viewer (version 1.6). A ×60 oil-immersion objective was used for scanning. Serial confocal optical sections were taken at a step size of 0.5 to 0.7 μm

SUPPLEMENTARY DATA

Supplemental Figure 1. RT-PCR analysis of SYT2 gene expression.

Supplemental Figure 2. Fluorometric and histochemical GUS assay of SYT2.

Supplemental Figure 3. SYT2 RNAi construct.

Supplemental Figure 4. Growth rates of pollen tubes of WT and *SYT*2 mutants.

Supplemental Figure 5. Subcellular localisation of SYT2-GFP, GFP and DsRed-E5.

Supplemental Figure 6. Immunofluorescence labelling in the pollen tubes showed that SYT2 was localised on the plasma membrane.

Supplemental Figure 7. BFA treatment results in enlarged compartments in *p35S:SYT2-GFP*-overexpressing *Arabidopsis thaliana* L. suspension cells.

Supplemental Figure 8. Na^{+}-independent phospholipid binding of SYT2.

Supplemental Figure 9. Mg^{2+}-independent phospholipid binding of SYT2.

Supplemental Table 1. Primers used in this study.

Supplemental Table 2. Pollen germination and growth rate of pollen tubes of WT and *SYT2* mutant.

Supplemental Table 3. *Arabidopsis thaliana* L. synaptotagmin gene family.

FUNDING

The work was supported by The National Natural Science Foundation of China (Granted No. 31070220 and 30771087), The National Basic Research Program of China (Granted No. 2013CB126902). Part of the work of W. S. and F. B. was supported by DAAD (German Academic Exchange Service). J.J, K.M, and J.T. were supported by the Research and Development Operational Program "Comenius University Science Park" (ERDF, ITMS 26240220086).

AUTHOR CONTRIBUTIONS

Conceptualization and Methodology, H.Z. and F.B.; Investigation, H.W., S.H., W.S., Q.S., Y.X., X.W., K.M., J.T., B.V., H.L., P.C., J.L. and H.Z.; Writing –

Original Draft, H.W., W.S., F.B and H.Z.; Writing – Review & Editing, Y.W.; Funding Acquisition, F.B. and H.Z.; Supervision, F.B., H.Z., Y.X. and J.J.

ACKNOWLEDGEMENTS

We thank Professor Haiyun Ren (Beijing Normal University, China) for the gifts of the pCAMBIA 1300.1 construct and *Arabidopsis thaliana* L. suspension cells and her laboratory personnel for their technical assistance. No conflict of interest declared.

FIGURE LEGENDS

Figure 1. *SYT2* shows a pollen-specific expression pattern in *Arabidopsis*.

(A) Real time PCR analysis of *SYT2* in the indicated tissues. R = root, St = stem, L = leaf, P = pollen, Si = silique. Error bars represent the standard errors (±SE) from three biological repeats.

(B) Histochemical detection of GUS activity in a *pSYT2:GUS* transgenic plant inflorescence. Bar=0.5 mm.

(C) Quantitative fluorometric analysis of *SYT2* promoter activity during flower development. The promoter showed maximum activity in 1.5-mm-long flower buds shortly before anthesis (arrow in Fig. 1B). Flowers 2 mm long represent fully opened flowers (arrowhead in Fig. 1B); 3 mm and 4 mm represent the length of siliques. Ten plants were analysed for two independent biological repeats. The fluorescence intensity of the stages was normalised to that of 1.5-mm-long flower buds. Error bars represent ±SEs of the mean (n=10).

(D) Quantitative fluorometric determination of promoter strength in pistils, stamens and the remainder of the flower buds were analysed shortly before anthesis. The fluorescence intensity of different parts was normalised to that of the intact flower buds. AN = anther, CA = carpel and RE = remainder of flower parts. Error bars represent ±SEs of the mean (n=10).

(E) Histochemical localisation of GUS activity in ovules (arrows represent female gametophytes). Bar=20 μm.

(F) Histochemical staining of GUS activity in developing and matured pollen grains. Bar=100 μm.

(G) Histochemical staining of GUS activity in pollen tubes grown on medium. Bar=15 μm.

(H) Histochemical assay of GUS activity in transgenic pollen tubes penetrating the pistil stigma of wild flowers (arrow). Ovules remained stainless after pollination (arrowheads). Wild-type flower buds were emasculated, pollinated by transgenic pollen grains and examined after 24 h. Bar=100 μm.

(I) Histochemical assay of GUS activity in pistils of transgenic plants after pollination with wild-type pollen grains. Emasculated flower buds were left to develop mature ovules for 24h, then pollinated with a few wild type pollen grains and stained after 24 h. Signal disappeared from fertilised growing ovules (arrow), while unfertilised ovules remained small and stained strongly (arrowhead). Bar=100 μm.

(J) Histochemical assay of GUS activity in emasculated transgenic flowers. Flower buds were emasculated and a histochemical assay was conducted after 24 h. Bar=100 μm.

Figure 2. *SYT2* mutants show reduced germination rate and pollen tube length.

(A) Schematic diagram of *SYT2* gene structure and three T-DNA insertion lines (*syt2-1*, *syt2-2* and *syt2-3*). Black boxes indicate exons and lines between black boxes, introns. P1 (forward) and P2 (reverse) are primers for *syt2-1* diagnostic PCR. P1' (forward) and P2' (reverse) are primers for diagnostic PCRs of *syt2-2* and *syt2-3*. LBb1.3 is the primer specific to the T-DNA. RT Fw and RT Rev represent primers used for RT-PCR analysis. aa, amino acids.

(B) PCR analysis of the three T-DNA insertion lines. M: DNA molecular-weight markers. Primers used for PCR are indicated and shown in (A).

(C) *SYT2* expression analysis of three T-DNA insertion lines (*syt2-1*, *syt2-2*,

syt2-3) and one RNAi mutant (*RNAi-#5*). To compare *SYT2* to *SYT1, SYT1* was used as a positive control. The *Actin2* gene was used as an internal control.

(D) Relative pollen germination efficiency of Col-0 and *SYT2* mutants. The upper panel shows micrographs of pollen grains and pollen tubes of the wild-type (Col-WT) and *syt2* mutant lines (*syt2-1*, *syt2-2*, *syt2-3*, and *RNAi-#5*). Germination percentage of pollen from wild-type plants is defined as 100%. The histogram shows the relative germination efficiency of the pollen grains (Student's t-test, $*p < 0.05$, $**p < 0.001$). Error bars represent ±SE ($n \geq 70$) from three independent experiments.

(E) Pollen tube lengths and frequency distributions of different tube lengths. The upper histogram shows the pollen tube lengths of the wild-type and mutants. The pollen tube lengths of mutants were shorter than those of the wild type (Mann-Whitney U test; $**p < 0.001$). All pollen grains were geminated *in vitro* for 5 h. Error bars represent ±SE ($n \geq 200$) from three biological repeats. The stacked bar chart below shows the statistical frequency distribution of pollen tubes lengths < 55 µm, 55-95 µm, and > 95 µm. Bar colours represent tube length: yellow, > 95 µm; green, 55-95 µm; and blue, < 55 µm. Error bars represent ±SE ($n \geq 200$) from three biological repeats.

Figure 3. SYT2-GFP localises to the Golgi apparatus in the pollen tubes of transformed tobacco and *Arabidopsis* lines.

(A) SYT2-GFP driven by the *LAT52* promoter showed no co-localisation either with endocytic vesicles labelled with 2 µM of FM4-64 (30 min) or with ER lumen labelled with 100 nM of ER-Tracker Blue-White DPX (20 min) but the co-localisation with the Golgi apparatus labelled respectively with 5 µM of C5 Ceramide (1 h) and the Golgi marker (GmMan1-mCh) in *Arabidopsis thaliana* L. pollen tubes. Bars = 10 µm.

(B) SYT2-GFP aggregated and surrounded the FM4-64-stained BFA bodies (arrow heads) after 35.6 µM of BFA treatment (30 min), but did not incorporate into the FM4-64-stained wortmannin-induced compartment (arrow) after 10 µM

of wortmannin treatment (30 min) in *Arabidopsis thaliana* L. pollen tubes. Bars = 10 µm.

(C) SYT2-GFP showed no co-localisation with FM4-64 (2 µM, 10 min)-stained endocytic vesicles, but overlapped with C5 Ceramide (5 µM, 1 h)-stained Golgi apparatus in tobacco (*Nicotiana tabacum* L.) pollen tubes. Bars = 5 µm.

Figure 4. SYT2-DsRed-E5 localises at both the plasma membrane and distinct patches in *Arabidopsis thaliana* L. suspension cells.

(A) Subcellular localisation of SYT2 in *p35S:SYT2-DsRED-E5 Arabidopsis thaliana* L. suspension cells. A quantity of 5 mg/L of Hoechst33342 was used to stain nuclei for 10 min. Vesicles around the nucleus (blue) show green (GF) and red (RF) fluorescence. The plasma membrane shows only RF. Arrows indicate the fluorescent lines on the cell periphery.

(B) Z-stack projection of (A). This image is derived from stacks of 10 sections. The arrows in (A) and (B) indicate SYT2 vesicles close to the plasma membrane. Arrows indicate the fluorescent lines on the cell periphery.

(C) No fluorescence was found on trans-vacuolar cytoplasmic strands or the tonoplast. Arrows indicate the non-fluorescent trans-vacuolar cytoplasmic strands.

(D) Plasmolysis of *p35S:SYT2-DsRED-E5 Arabidopsis thaliana* L. suspension cell shows no fluorescence on the cell wall. Arrows parallel with an asterisk indicate the cell wall, while arrows parallel with two asterisks indicate the plasma membrane.

Bars = 10 µm.

Figure 5. Protein dynamics analysis of SYT2 using the DsRED-E5 fluorescence timer.

(A) Grayscale images of DsRED-E5 and SYT2-DsRED-E5 green and red fluorescence signals. Aa, the control DsRED-E5 fluorescence shows green and red fluorescence signals of similar intensities. Ab and Ac, SYT2-DsRED-E5 signals on the vesicles around the nucleus (V_1), and on the vesicles close to (V_2) and on (M) the plasma membrane. Bars=10 µm.

(B) Analysis of the green/red fluorescence ratio using control DsRED-E5 and SYT2-DsRED-E5 proteins. The green fluorescence of V_1 and V_2 is stronger than red fluorescence (GF/RF>1), while the red fluorescence on the plasma membrane (M) is stronger than green fluorescence (GF/RF<1). To measure the V1 and V2 fluorescence signals, 15 cells were analysed and five vesicles were chosen randomly from each cell for statistical analysis. Error bars represent SE (n=75).

Figure 6. BFA treatment prevents SYT2-DeRED-E5 transfer to the plasma membrane in *p35S:SYT2-DsRED-E5*-overexpressing *Arabidopsis thaliana* L. suspension cells

(A) *p35S:SYT2-DsRED-E5*-overexpressing *Arabidopsis thaliana* L. suspension cells without BFA treatment. Vesicles (V_0) showed predominantly green fluorescence, while the plasma membrane (M_0) showed predominantly red fluorescence. Bar=5 μm.

(B) *Arabidopsis thaliana* L. suspension cells stably expressing SYT2-DsRED-E5 were treated with 50 μM BFA for 20 min. Bar=5 μm.

(C) *Arabidopsis thaliana* L. suspension cells stably expressing SYT2-DsRED-E5 were treated with 50 μM BFA for 40 min. SYT2-positive vesicles (V_{40}) aggregate to larger compartments. Vesicles (V_{40}) showed stronger green fluorescence signals, while the plasma membrane (M_{40}) showed weaker red fluorescence signals. Bar = 5 μm.

(D) Analyses of the green and red fluorescence ratio of SYT2-DsRED-E5 protein after BFA treatment. V_0 indicates vesicles without BFA treatment and M_0 indicates plasma membrane without BFA treatment. V_{20} and M_{20} indicate 20 min of BFA treatment; V_{40} and M_{40} indicate 40 min of BFA treatment. Initially, the green fluorescence on V_0 was stronger than the red fluorescence (GF/RF>1), while the red fluorescence on M_0 was stronger than the green fluorescence (GF/RF<1). There was no obvious difference in the GF/RF ratio between V_0 and V_{20}; however, the GF/RF ratio of V_{40} was significantly different from that of V_0 (t-test, *p<0.05). Compared with M_0, the RF/GF ratios of M_{20}

and M_{40} were significantly increased (t-test, *p<0.05 and **p<0.01, respectively). To measure the fluorescence signals, 10 cells of each group were analysed, and five vesicles were chosen randomly from each cell for statistical analysis. Error bars represented ±SE (n=70).

Figure 7. SYT2$^{\Delta C2AB}$-GFP/DsRed-E5 lacking C2AB domains of SYT2 localises to the Golgi apparatus in *Arabidopsis thaliana* L. suspension cells.

(A) SYT2-GFP localised on the Golgi apparatus, but not all C5 ceramide-stained signals overlapped with SYT2-GFP.

(B) The C-terminal tagged SYT2$^{\Delta C2AB}$-GFP lacking C2AB domains showed a punctate distribution, and was localised to the C5 ceramide-stained Golgi apparatus.

(C) SYT2$^{\Delta C2AB}$-DsRED-E5 localised to the Golgi apparatus, but not the plasma membrane.

Bars = 10 μm.

Figure 8. Ca^{2+}- dependent phospholipid binding of SYT2.

C2A domain (A), The C2B domain (B) and C2AB domains (C) of SYT2 were incubated with liposomes in the presence of the indicated concentrations of free Ca^{2+} (clamped with Ca^{2+}/EGTA buffers) to estimate partial binding of free Ca^{2+}. The amino acid residues at positions 244 to 400 represent the C2A domain of SYT2, 401 to 537 represent the C2B domain of SYT2, and 247 to 537 represent the C2AB domain of SYT2. Purified GST fusion proteins containing the corresponding residues of SYT2 C2 domains were incubated in various concentrations of free Ca^{2+} with liposomes composed of 25% PS/75% PC. Liposomes were precipitated by centrifugation, and bound proteins were analysed by SDS-PAGE. The EC_{50} for C2AB was 2–3 μM. Error bars represent ±SE (n=3).

REFERENCES

Apodaca, G. (2006). Synaptotagmins: mediators of Ca^{2+}-regulated vesicle fusion. Focus on "stable gene

857 silencing of synaptotagmin Ⅰ in rat PC12 cells inhibits Ca^{2+}-evoked release of
858 catecholamine". Am J Physiol Cell Physiol 291:C234-236.
859 Baird, G.S., Zacharias, D.A., and Tsien, R.Y. (2000). Biochemistry, mutagenesis, and oligomerization
860 of DsRed, a red fluorescent protein from coral. Proc Natl Acad Sci U S A 97:11984-11989.
861 Bhalla, A., Chicka, M.C., and Chapman, E.R. (2008). Analysis of the synaptotagmin family during
862 reconstituted membrane fusion. Uncovering a class of inhibitory isoforms. J Biol Chem
863 283:21799-21807.
864 Bozkurt, T.O., Richardson, A., Dagdas, Y.F., Mongrand, S., Kamoun, S., and Raffaele, S. (2014). The
865 Plant Membrane-Associated REMORIN1.3 Accumulates in Discrete Perihaustorial Domains
866 and Enhances Susceptibility to Phytophthora infestans. Plant Physiol 165:1005-1018.
867 Brose, N., Petrenko, A.G., Sudhof, T.C., and Jahn, R. (1992). Synaptotagmin: a calcium sensor on the
868 synaptic vesicle surface. Science 256:1021-1025.
869 Caler, E.V., Chakrabarti, S., Fowler, K.T., Rao, S., and Andrews, N.W. (2001). The
870 Exocytosis-regulatory protein synaptotagmin Ⅶ mediates cell invasion by Trypanosoma
871 cruzi. J Exp Med 193:1097-1104.
872 Camacho, L., and Malhó, R. (2003). Endo/exocytosis in the pollen tube apex is differentially regulated
873 by Ca^{2+} and GTPases. J Exp Bot 54:83-92.
874 Chae, K., and Lord, E.M. (2011). Pollen tube growth and guidance: roles of small, secreted proteins.
875 Annals of Botany 108:627-636.
876 Chapman, E.R. (2002). Synaptotagmin: a Ca^{2+} sensor that triggers exocytosis? Nat Rev Mol Cell Biol
877 3:498-508.
878 Chen, C.Y., Wong, E.I., Vidali, L., Estavillo, A., Hepler, P.K., Wu, H.M., and Cheung, A.Y. (2002). The
879 regulation of actin organization by actin-depolymerizing factor in elongating pollen tubes.
880 Plant Cell 14:2175-2190.
881 Chen, H., Chou, M., Wang, X., Liu, S., Zhang, F., and Wei, G. (2013). Profiling of differentially
882 expressed genes in roots of Robinia pseudoacacia during nodule development using
883 suppressive subtractive hybridization. PLoS One 8:e63930.
884 Chen, J., Gutjahr, C., Bleckmann, A., and Dresselhaus, T. (2015). Calcium Signaling during
885 Reproduction and Biotrophic Fungal Interactions in Plants. Mol Plant 8:595-611.
886 Cho, W., and Stahelin, R.V. (2006). Membrane binding and subcellular targeting of C2 domains.

887 Biochim Biophys Acta 1761:838-849.

888 Chudakov, D.M., Matz, M.V., Lukyanov, S., and Lukyanov, K.A. (2010). Fluorescent Proteins and
889 Their Applications in Imaging Living Cells and Tissues. Physiol Rev 90:1103-1163.

890 Coelho, P.C., and Malhó, R. (2006). Correlative Analysis of $[Ca^{2+}]_C$ and Apical Secretion during Pollen
891 Tube Growth and Reorientation. Plant Signal Behav 1:152-157.

892 Coussens, L., Parker, P.J., Rhee, L., Yang-Feng, T.L., Chen, E., Waterfield, M.D., Francke, U., and
893 Ullrich, A. (1986). Multiple, distinct forms of bovine and human protein kinase C suggest
894 diversity in cellular signaling pathways. Science 233:859-866.

895 Craxton, M. (2004). Synaptotagmin gene content of the sequenced genomes. BMC Genomics 5:43.

896 Craxton, M. (2007). Evolutionary genomics of plant genes encoding N-terminal-TM-C2 domain
897 proteins and the similar FAM62 genes and synaptotagmin genes of metazoans. BMC
898 Genomics 8:259.

899 Davidi, L., Levin, Y., Ben-Dor, S., and Pick, U. (2015). Proteome analysis of cytoplasmatic and of
900 plastidic beta-carotene lipid droplets in Dunaliella bardawil. Plant Physiol 167:60-79..

901 Dhonukshe, P., and Gadella, T.W., Jr. (2003). Alteration of microtubule dynamic instability during
902 preprophase band formation revealed by yellow fluorescent protein-CLIP170 microtubule
903 plus-end labeling. Plant Cell 15:597-611.

904 Duran, J.M., Anjard, C., Stefan, C., Loomis, W.F., and Malhotra, V. (2010). Unconventional secretion
905 of Acb1 is mediated by autophagosomes. J Cell Biol 188:527-536.

906 Fan, L.M., Wang, Y.F., Wang, H., and Wu, W.H. (2001). In vitro Arabidopsis pollen germination and
907 characterization of the inward potassium currents in Arabidopsis pollen grain protoplasts. J
908 Exp Bot 52:1603-1614.

909 Fernandez-Chacon, R., Shin, O.H., Konigstorfer, A., Matos, M.F., Meyer, A.C., Garcia, J., Gerber, S.H.,
910 Rizo, J., Sudhof, T.C., and Rosenmund, C. (2002). Structure/function analysis of Ca^{2+} binding
911 to the C2A domain of synaptotagmin 1. J Neurosci 22:8438-8446.

912 Fernandez, I., Arac, D., Ubach, J., Gerber, S.H., Shin, O., Gao, Y., Anderson, R.G., Sudhof, T.C., and
913 Rizo, J. (2001). Three-dimensional structure of the synaptotagmin 1 C2B-domain:
914 synaptotagmin 1 as a phospholipid binding machine. Neuron 32:1057-1069.

915 Fukuda, M., Kowalchyk, J.A., Zhang, X., Martin, T.F., and Mikoshiba, K. (2002). Synaptotagmin Ⅸ
916 regulates Ca^{2+}-dependent secretion in PC12 cells. J Biol Chem 277:4601-4604.

917 Ge, L.L., Tian, H.Q., and Russell, S.D. (2007). Calcium function and distribution during fertilization in
918 angiosperms. Am J Bot 94:1046-1060.
919 Geppert, M., Goda, Y., Hammer, R.E., Li, C., Rosahl, T.W., Stevens, C.F., and Sudhof, T.C. (1994).
920 Synaptotagmin Ⅰ: a major Ca^{2+} sensor for transmitter release at a central synapse. Cell
921 79:717-727.
922 Gu, Y., Vernoud, V., Fu, Y., and Yang, Z. (2003). ROP GTPase regulation of pollen tube growth through
923 the dynamics of tip-localized F-actin. J Exp Bot 54:93-101.
924 Guan, K.L., and Dixon, J.E. (1991). Eukaryotic proteins expressed in *Escherichia coli*: an improved
925 thrombin cleavage and purification procedure of fusion proteins with glutathione S-transferase.
926 Anal Biochem 192:262-267.
927 Gustavsson, N., Wei, S.H., Hoang, D.N., Lao, Y., Zhang, Q., Radda, G.K., Rorsman, P., Sudhof, T.C.,
928 and Han, W. (2009). Synaptotagmin-7 is a principal Ca^{2+} sensor for Ca^{2+} -induced glucagon
929 exocytosis in pancreas. J Physiol 587:1169-1178.
930 Helling, D., Possart, A., Cottier, S., Klahre, U., and Kost, B. (2006). Pollen tube tip growth depends on
931 plasma membrane polarization mediated by tobacco PLC3 activity and endocytic membrane
932 recycling. Plant Cell 18:3519-3534.
933 Hepler, P.K., Vidali, L., and Cheung, A.Y. (2001). Polarized cell growth in higher plants. Annu Rev
934 Cell Dev Biol 17:159-187.
935 Iezzi, M., Eliasson, L., Fukuda, M., and Wollheim, C.B. (2005). Adenovirus-mediated silencing of
936 synaptotagmin 9 inhibits Ca^{2+}-dependent insulin secretion in islets. FEBS Lett 579:5241-5246.
937 Iezzi, M., Kouri, G., Fukuda, M., and Wollheim, C.B. (2004). Synaptotagmin Ⅴ and Ⅸ isoforms
938 control Ca^{2+} -dependent insulin exocytosis. J Cell Sci 117:3119-3127.
939 Jahn, R., Lang, T., and Sudhof, T.C. (2003). Membrane fusion. Cell 112:519-533.
940 Jaiswal, J.K., Chakrabarti, S., Andrews, N.W., and Simon, S.M. (2004). Synaptotagmin Ⅶ restricts
941 fusion pore expansion during lysosomal exocytosis. PLoS Biol 2:E233.
942 Jefferson, R.A., Kavanagh, T.A., and Bevan, M.W. (1987). GUS fusions: beta-glucuronidase as a
943 sensitive and versatile gene fusion marker in higher plants. EMBO J 6:3901-3907.
944 Koh, T.W., and Bellen, H.J. (2003). Synaptotagmin I, a Ca^{2+} sensor for neurotransmitter release. Trends
945 Neurosci 26:413-422.
946 Lalanne, E., Honys, D., Johnson, A., Borner, G.H., Lilley, K.S., Dupree, P., Grossniklaus, U., and Twell,

D. (2004). *SETH1* and *SETH2*, two components of the glycosylphosphatidylinositol anchor biosynthetic pathway, are required for pollen germination and tube growth in Arabidopsis. Plant Cell 16:229-240.

Leitzell, K. (2007). Synaptotagmin: is 2 better than 1? J Neurosci 27:4231-4232.

Lewis, J.D., and Lazarowitz, S.G. (2010). Arabidopsis synaptotagmin SYTA regulates endocytosis and virus movement protein cell-to-cell transport. Proc Natl Acad Sci U S A 107:2491-2496.

Lu, Y.J., Schornack, S., Spallek, T., Geldner, N., Chory, J., Schellmann, S., Schumacher, K., Kamoun, S., and Robatzek, S. (2012). Patterns of plant subcellular responses to successful oomycete infections reveal differences in host cell reprogramming and endocytic trafficking. Cell Microbiol 14:682-697.

Martens, S., Kozlov, M.M., and McMahon, H.T. (2007). How synaptotagmin promotes membrane fusion. Science 316:1205-1208.

Martinez, I., Chakrabarti, S., Hellevik, T., Morehead, J., Fowler, K., and Andrews, N.W. (2000). Synaptotagmin Ⅶ regulates Ca^{2+}-dependent exocytosis of lysosomes in fibroblasts. J Cell Biol 148:1141-1149.

Minami, A., Fujiwara, M., Furuto, A., Fukao, Y., Yamashita, T., Kamo, M., Kawamura, Y., and Uemura, M. (2009). Alterations in detergent-resistant plasma membrane microdomains in Arabidopsis thaliana during cold acclimation. Plant cell physiol 50:341-359.

Mirabella, R., Franken, C., van der Krogt, G.N., Bisseling, T., and Geurts, R. (2004). Use of the fluorescent timer DsRED-E5 as reporter to monitor dynamics of gene activity in plants. Plant Physiol 135:1879-1887.

Moscatelli, E.O., and Alessandra. (2013). Endocytic Pathways and Recycling in Growing Pollen Tubes. Plants 2:211-229.

Nelson, B.K., Cai, X., and Nebenfuhr, A. (2007). A multicolored set of in vivo organelle markers for co-localization studies in Arabidopsis and other plants. Plant J 51:1126-1136.

Nicot, N., Hausman, J.F., Hoffmann, L., and Evers, D. (2005). Housekeeping gene selection for real-time RT-PCR normalization in potato during biotic and abiotic stress. J Exp Bot 56:2907-2914.

Pang, Z.P., Melicoff, E., Padgett, D., Liu, Y., Teich, A.F., Dickey, B.F., Lin, W., Adachi, R., and Sudhof, T.C. (2006). Synaptotagmin-2 is essential for survival and contributes to Ca^{2+} triggering of

neurotransmitter release in central and neuromuscular synapses. J Neurosci 26:13493-13504.

Perez Sancho, J., Vanneste, S., Lee, E., McFarlane, H., Esteban del Valle, A., Valpuesta, V., Friml, J., Botella, M.A., and Rosado, A. (2015). The Arabidopsis SYT1 is enriched in ER-PM contact sites and confers cellular resistance to mechanical stresses. Plant Physiol 168:132-143.

Pierson, E.S., Miller, D.D., Callaham, D.A., Shipley, A.M., Rivers, B.A., Cresti, M., and Hepler, P.K. (1994). Pollen tube growth is coupled to the extracellular calcium ion flux and the intracellular calcium gradient: effect of BAPTA-type buffers and hypertonic media. Plant Cell 6:1815-1828.

Reddy, A., Caler, E.V., and Andrews, N.W. (2001). Plasma membrane repair is mediated by Ca^{2+}-regulated exocytosis of lysosomes. Cell 106:157-169.

Rose, C.M., Venkateshwaran, M., Volkening, J.D., Grimsrud, P.A., Maeda, J., Bailey, D.J., Park, K., Howes-Podoll, M., den Os, D., Yeun, L.H., et al. (2012). Rapid phosphoproteomic and transcriptomic changes in the rhizobia-legume symbiosis. Mol Cell Proteomics 11:724-744.

Sanford, J.C., Smith, F.D., and Russell, J.A. (1993). Optimizing the biolistic process for different biological applications. Methods Enzymol 217:483-509.

Schapire, A.L., Voigt, B., Jasik, J., Rosado, A., Lopez-Cobollo, R., Menzel, D., Salinas, J., Mancuso, S., Valpuesta, V., Baluska, F., et al. (2008). Arabidopsis synaptotagmin 1 is required for the maintenance of plasma membrane integrity and cell viability. Plant Cell 20:3374-3388.

Shin, O.H., Rhee, J.S., Tang, J., Sugita, S., Rosenmund, C., and Sudhof, T.C. (2003). Sr^{2+} binding to the Ca^{2+} binding site of the synaptotagmin 1 C2B domain triggers fast exocytosis without stimulating SNARE interactions. Neuron 37:99-108.

Sutton, R.B., Davletov, B.A., Berghuis, A.M., Sudhof, T.C., and Sprang, S.R. (1995). Structure of the first C2 domain of synaptotagmin I: a novel Ca^{2+}/phospholipid-binding fold. Cell 80:929-938.

Szumlanski, A.L., and Nielsen, E. (2009). The Rab GTPase RabA4d Regulates Pollen Tube Tip Growth in Arabidopsis thaliana. Plant Cell 21:526-544.

Takahashi, D., Kawamura, Y., and Uemura, M. (2013). Detergent-resistant plasma membrane proteome to elucidate microdomain functions in plant cells. Frontiers in plant science 4:27.

Terskikh, A., Fradkov, A., Ermakova, G., Zaraisky, A., Tan, P., Kajava, A.V., Zhao, X., Lukyanov, S., Matz, M., Kim, S., et al. (2000). "Fluorescent timer": protein that changes color with time. Science 290:1585-1588.

1007 Terskikh, A.V., Fradkov, A.F., Zaraisky, A.G., Kajava, A.V., and Angres, B. (2002). Analysis of DsRed
1008 Mutants: SPACE AROUND THE FLUOROPHORE ACCELERATES FLUORESCENCE
1009 DEVELOPMENT. J Biol Chem 277:7633-7636.
1010 Thorlby, G., Fourrier, N., and Warren, G. (2004). The SENSITIVE TO FREEZING2 gene, required for
1011 freezing tolerance in *Arabidopsis thaliana*, encodes a beta-glucosidase. Plant Cell
1012 16:2192-2203.
1013 Tucker, W.C., and Chapman, E.R. (2002). Role of synaptotagmin in Ca^{2+}-triggered exocytosis.
1014 Biochem J 366:1-13.
1015 Tucker, W.C., Weber, T., and Chapman, E.R. (2004). Reconstitution of Ca^{2+}-regulated membrane fusion
1016 by synaptotagmin and SNAREs. Science 304:435-438.
1017 Uchiyama, A., Shimada-Beltran, H., Levy, A., Zheng, J.Y., Javia, P.A., and Lazarowitz, S.G. (2014).
1018 The Arabidopsis synaptotagmin SYTA regulates the cell-to-cell movement of diverse plant
1019 viruses. Frontiers in plant science 5:584.
1020 Wang, C., Shang, J.X., Chen, Q.X., Oses-Prieto, J.A., Bai, M.Y., Yang, Y., Yuan, M., Zhang, Y.L., Mu,
1021 C.C., Deng, Z., et al. (2013). Identification of BZR1-interacting proteins as potential
1022 components of the brassinosteroid signaling pathway in Arabidopsis through tandem affinity
1023 purification. Mol Cell Proteomics 12:3653-3665.
1024 Xu, J., Mashimo, T., and Sudhof, T.C. (2007). Synaptotagmin-1, -2, and -9: Ca^{2+} sensors for fast release
1025 that specify distinct presynaptic properties in subsets of neurons. Neuron 54:567-581.
1026 Yamazaki, T., Kawamura, Y., Minami, A., and Uemura, M. (2008). Calcium-dependent freezing
1027 tolerance in Arabidopsis involves membrane resealing via synaptotagmin SYT1. Plant Cell
1028 20:3389-3404.
1029 Yamazaki, T., Takata, N., Uemura, M., and Kawamura, Y. (2010). Arabidopsis synaptotagmin SYT1, a
1030 type I signal-anchor protein, requires tandem C2 domains for delivery to the plasma
1031 membrane. J Biol Chem 285:23165-23176.
1032 Yarbrough, D., Wachter, R.M., Kallio, K., Matz, M.V., and Remington, S.J. (2001). Refined crystal
1033 structure of DsRed, a red fluorescent protein from coral, at 2.0-Å resolution. Proc Natl Acad
1034 Sci U S A 98:462-467.
1035 Zarsky, V., Cvrckova, F., Potocky, M., and Hala, M. (2009). Exocytosis and cell polarity in plants -
1036 exocyst and recycling domains. New Phytol 183:255-272.

1037 Zhang, H., Zhang, L., Gao, B., Fan, H., Jin, J., Botella, M.A., Jiang, L., and Lin, J. (2011). Golgi
1038 apparatus-localized synaptotagmin 2 is required for unconventional secretion in Arabidopsis.
1039 PLoS One 6:e26477.
1040 Zimmermann, P., Hirsch-Hoffmann, M., Hennig, L., and Gruissem, W. (2004). GENEVESTIGATOR.
1041 Arabidopsis Microarray Database and Analysis Toolbox. Plant Physiol 136:2621-2632.
1042